Density-wave-type supersolid of two-dimensional tilted dipolar bosons

A. N. Aleksandrova [1], I. L. Kurbakov [2], A. K. Fedorov [3,4,*] and Yu. E. Lozovik [2,3,5,†]

[1] *Moscow Pedagogical State University, Moscow 119991, Russia*

[2] *Institute of Spectroscopy, Russian Academy of Sciences, Troitsk, Moscow 142190, Russia*

[3] *Russian Quantum Center, Skolkovo, Moscow 121205, Russia*

[4] *National University of Science and Technology MISIS, Moscow 119049, Russia*

[5] *National Research University Higher School of Economics, Moscow 109028, Russia*

(Received 12 December 2023; revised 14 May 2024; accepted 28 May 2024; published 24 June 2024)

We predict a stable density-wave-type supersolid phase of a dilute gas of tilted dipolar bosons in a two-dimensional (2D) geometry. This many-body phase is manifested by the formation of the stripe pattern and elasticity coexisting together with the Bose-Einstein condensation and superfluidity at zero temperature. With the increasing of the tilting angle the type of the gas-supersolid transition changes from the first order to the second-order one despite the 2D character of the system, whereas the anisotropy and many-body stabilizing interactions play crucial roles. Our approach is based on the numerical analysis of the phase diagram using the simulated annealing method for a free-energy functional. The predicted supersolid effect can be realized in a variety of experimental setups ranging from excitons in heterostructures to cold atoms and polar molecules in optical potentials.

DOI: 10.1103/PhysRevA.109.063326

I. INTRODUCTION

Remarkable progress on creating ultracold clouds of diatomic polar molecules [1–3], degenerate gases of large-spin atoms [4–7], and long-lived excitons in solid-state systems [8–14] makes it realistic to observe a large variety of interesting phenomena in dipolar systems and confirm seminal theoretical predictions [15–19] (for a review, see Refs. [20–24]). Among nonconventional many-body phases of ultracold matter, a supersolid state attracts special attention [25–30]. In such an unusual state, the condensate wave function has a lattice structure on top of a uniform background [31–35]. In addition to ultracold dipolar gases, supersolidity takes place in a range of systems, such as two-component systems [36], Bose-Fermi mixtures [37], and condensates in optical lattices [38,39].

There are several mechanisms for the realization of supersolidity in ultracold quantum dipolar gases. Dilute weakly interacting dipolar gases of bosons in two dimensions may demonstrate the roton-maxon structure of the spectrum by fine-tuning the short-range part of the interaction potential [40]. It is then possible to achieve vanishing the roton gap, the so-called the roton instability regime, where the system is unstable with respect to periodic modulations of the order parameter [34]. However, instead of forming a supersolid state when approaching the roton instability, the condensate depletion diverges [41–43]. One of the possible ways to avoid this divergence has been suggested in the case of tilted dipoles with the anisotropy of the excitation spectrum [44]. Alternatively, the supersolid state of dipolar bosons can be rallied in the dense (strongly correlated) regime [45–48], in which the corresponding crystal has one particle per lattice site [49,50]. In this regime the supersolid state is possible in the presence of thermodynamically nonequilibrium defects in crystals only [51]. The presence of this phenomenon has been confirmed numerically [52–56] and in experiments [57,58].

Nevertheless, one of the most intriguing questions relates to the possibility to obtain supersolidity in the dilute regime, where the mean-field description of the dilute trapped dipolar degenerate gases may be still valid [41,59,60]. The crucial requirement for obtaining supersolidity in the dilute regime is stabilizing the system [61,62], which can be achieved, for example, by adding a three-body repulsion [35]. Without taking into account the many-body stabilization, the supersolid state can be considered as transient [63]. Recent advances in the study of supersolids of quantum gases are related to probing the roton excitation spectrum [64–67], forming quantum stripes or droplets maintaining phase coherence [68–71], and eventually experimental observing supersolidity [67]. A complimentary mechanism for forming supersolidity in a dipolar quantum gas is related to the aforementioned anisotropy with respect to the rotational symmetry for a system of tilted dipoles, which leads to the convergence of the condensate depletion up to the threshold of the roton instability [44]. The latter approach to forming supersolid states has a potential advantage in the form of an additional level of controllability, which is possible by manipulating the tilting angle of dipoles.

We note that two-dimensional (2D) systems of tilted dipoles and the formation of stripe phases have been studied via numerics yielding varying conclusions about the presence (or absence) of the striped supersolid phase [72–75]. However, details of numerical approaches and magnitudes of statistical

*Contact author: akf@rqc.ru

†Contact author: lozovik@isan.troitsk.ru

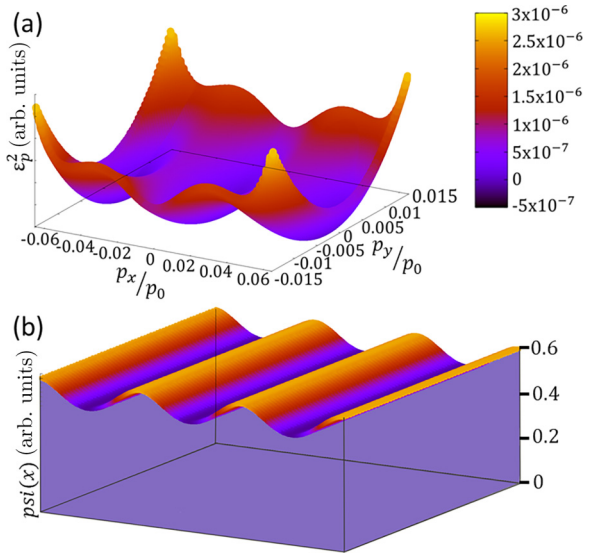

FIG. 1. Supersolid state of a two-dimensional dilute gas of dipolar bosons. In panel (a), the 2D anisotropic excitation spectrum of the system when the roton gap is vanishing, which leads to the instability of the homogeneous phase, is shown. In panel (b), the 2D order parameter in the real space with the signatures of the density-wave-type supersolid is illustrated ($p_0 = 2\pi\hbar\sqrt{n_{\rm av}}$, the dimensionless parameter is $\alpha_3 = 0.402$ and the tilting angle is $\theta = 46^\circ$; for details, see Sec. III).

errors may influence the conclusion [76,77], so additional analytical approaches are required to study the striped supersolid phase. We also note that aforementioned works have considered both zero and nonzero temperatures, whereas our consideration below is for the zero-temperature case only.

In this work, we solve the Gross-Pitaevskii (GP) equation by means of a straightforward minimization for the GP (i.e., free-energy) functional. We consider a 2D system of tilted dipoles in a finite-thickness layer [44] under a stabilization by many-body effects [61]. As many-body effects, we employ both externally imposed three-body interactions [35,78] and the Lee-Huang-Yang (LHY) correction for dilute dipolar systems [79,80]. Remarkably, both methodologies yield qualitatively identical outcomes. We predict a stable density-wave-type supersolid state of a 2D dilute Bose-Einstein-condensed (BEC) gas of tilted dipoles. We obtain the full phase diagram of the system with both first and second kinds of the transition. We demonstrate the coexistence of superfluidity with elasticity and the crystalline stripe pattern at zero temperature (see Fig. 1 for the illustration), indicating the density-wave-type supersolid phase, which is possible due to the smallness of the condensate depletion [44].

Our paper is organized as follows. In Sec. II, we introduce the model of tilted dipolar bosons in a thin 2D layer and the stabilization by three-body interaction, with basic quantities of interest being defined. The technique that we use is based on the numerical minimization of the energy functional using stimulated annealing. In Sec. III, we present the results of the numerical investigation for such a model and observe numerically the evidence of a density-wave-type supersolid phase. In Sec. IV, we employ the same approach, but with many-body stabilization achieved through the LHY correction, yielding qualitatively similar results. We summarize our results in Sec. V.

II. TILTED DIPOLAR BOSONS: GENERAL RELATIONS

In this work, we consider a 2D BEC gas of tilted dipoles (for the detailed description of the system, see Ref. [44]). We consider the corresponding free-energy functional in the following form:

$$F[\psi(\mathbf{r})] - \mu N = \int \left[\psi^*(\mathbf{r}) \left[\frac{(-i\hbar\nabla + m\mathbf{v})^2}{2m} - \mu \right] \psi(\mathbf{r}) + e_0(|\psi(\mathbf{r})|^2) \right] d\mathbf{r} + \frac{1}{2} \int U(\mathbf{r}-\mathbf{s}) |\psi(\mathbf{r})\psi(\mathbf{s})|^2 d\mathbf{r} d\mathbf{s}, \quad (1)$$

which accounts for the 2D system ($\mathbf{r} = \{x, y\}$ and $\mathbf{p} = \{p_x, p_y\}$) at zero temperature, $T = 0$, while maintaining a constant chemical potential μ. Here, $\psi(\mathbf{r})$ represents the order parameter, $N = \int |\psi(\mathbf{r})|^2 d\mathbf{r}$ is the particle number, m is the particle mass, and $\mathbf{v}$ is the velocity of the nondissipative current. The equation of state for the homogeneous phase with density $n = N/S$ is as follows:

$$e_0(n) = \frac{g_2}{2} n^2 + \frac{g_3}{6} n^3 + \cdots . \quad (2)$$

Therefore, it describes the energy of the ground state per unit area as a function of the density n. In Eq. (2), the term with g_3 yields the three-body interaction [35,78], serving as a good model for many-body stabilization [81]. An implementation with independently controlled two-body and three-body interactions can be achieved with a bilayer featuring tunneling between layers; for details, see Ref. [78]. The coupling constants are defined as follows:

$$g_2 = g_s + (3\cos^2\theta - 1) g_d, \quad g_s = \frac{2\sqrt{2\pi}\hbar^2}{m z_0} a_s, \quad g_d = \frac{2\sqrt{2\pi}\hbar^2}{m z_0} a_d. \quad (3)$$

Here g_2 represents the two-body interaction, g_s corresponds to the s-wave scattering, g_d denotes the dipole-dipole interaction. Additionally, θ stands for the tilting angle of dipoles with respect to the 2D plane, and $z_0 = \sqrt{\hbar/m\omega_z}$, where z_0 and $\hbar\omega_z$ correspond to the Gaussian of the wave function along the tight direction. In the 2D regime, z_0 and $\hbar\omega_z$ coincide with the trap oscillator length and frequency, while beyond the 2D regime, the calculation is described in Sec. IV.

The parameters a_s and $a_d = md^2/3\hbar^2$ represent the 3D s-wave and dipole-dipole scattering lengths, respectively, with d being the dipole moment of the particles; $S = \int d\mathbf{r} \to \infty$ denotes the area of the periodic quantization box. In the Fourier transform of the interparticle interaction $U(\mathbf{r})$,

$$U(\mathbf{r}) = \int U(\mathbf{p}) e^{i\mathbf{p}\mathbf{r}/\hbar} \frac{d\mathbf{p}}{(2\pi\hbar)^2}, \quad (4)$$

the momentum-dependent component in the following form has been distinctly isolated:

$$U(\mathbf{p}) \equiv \mathcal{U}(\mathbf{p}) - \mathcal{U}(0) = \int \mathcal{U}(\mathbf{r})(e^{-i\mathbf{p}\mathbf{r}/\hbar} - 1) d\mathbf{r}. \quad (5)$$

Here $\mathcal{U}(\mathbf{p}) = \int \mathcal{U}(\mathbf{r}) e^{-i\mathbf{p}\mathbf{r}/\hbar} d\mathbf{r}$ is the effective 2D interaction potential for the thin-layer motion [44], and normalization condition $U(0) = 0$ is imposed. This normalization arises from the fact that the momentum-independent contribution $U(0) = \int U(\mathbf{r}) d\mathbf{r} = 0$ has already been accounted for within the quantity $d^2 e_0(n)/dn^2$. For tilted dipoles we have the following (see Ref. [44]):

$$U(\mathbf{p}) = U_h(\mathbf{p}) \sin^2\theta + U_v(\mathbf{p}) \cos^2\theta, \tag{6}$$

$$U_h(\mathbf{p}) = \frac{4d^2}{\hbar} \int_0^\infty \frac{p_x^2 dp_z}{p_x^2 + p_y^2 + p_z^2} \exp\left(-\frac{p_z^2 z_0^2}{2\hbar^2}\right), \tag{7}$$

$$U_v(\mathbf{p}) = -\frac{4d^2}{\hbar} \int_0^\infty \frac{(p_x^2 + p_y^2) dp_z}{p_x^2 + p_y^2 + p_z^2} \exp\left(-\frac{p_z^2 z_0^2}{2\hbar^2}\right), \tag{8}$$

and, finally, we assume the two-dimensionality of the problem ($\hbar\omega_z \gg 4\pi\hbar^2 n/m$) and the weakly interacting regime ($g_s, g_d, g_3 n \ll 4\pi\hbar^2/m$).

A. Trial wave function and details of the minimization

The Bogoliubov excitation spectra,

$$\varepsilon_{\mathbf{p}} = \sqrt{T_{\mathbf{p}}(T_{\mathbf{p}} + 2U_{\mathbf{p}})},$$
$$T_{\mathbf{p}} \equiv \frac{p^2}{2m},$$
$$U_{\mathbf{p}} \equiv \left(\frac{d^2 e_0(n)}{dn^2} + U(\mathbf{p})\right) n, \tag{9}$$

of systems with the free-energy functional of the form given by Eq. (1) exhibit a roton-maxon effect along the y axis, as expressed by Eqs. (6)–(8), which is stronger than that along the x axis, i.e., $\varepsilon_{p,0} > \varepsilon_{0,p}$. As a result, the density wave (DW) in the emerging supersolid phase may be oriented along the x axis, with the vector aligned along the y axis. Consequently, as a trial function for the functional $F[\psi(\mathbf{r})] - \mu N$ [see Eq. (1)], we consider complex-valued functions that are periodic with a period λ, depending only on the variable y:

$$\psi(\mathbf{r}) \equiv \psi(y) = \psi(y + \lambda). \tag{10}$$

In the Fourier series expansion of functions $\psi(y)$, we consider a finite number of harmonics to achieve the desired accuracy. The function $e(|\psi(y)|^2)$ is integrated in the position representation. For the undeformed DW, we are looking for the global minimum of the functional with respect to both λ and the amplitudes of the harmonics. In the case of the deformed DW, the minimization is performed only with respect to the amplitudes of the harmonics. In the absence of the velocity, the function $\psi(y)$ is an even real function.

B. Computed quantities

For both phases, the homogeneous gas and the supersolid DW, we numerically compute a number of quantities.

(i) The compressibility

$$\frac{m^2}{\chi} = \frac{1}{\partial n/\partial\mu}. \tag{11}$$

(ii) The pressure

$$P = \mu n - \frac{F_0}{S}. \tag{12}$$

Here, $F_0 = F[\psi_0(y)]$ represents the value of the functional F, when $F - \mu N$ reaches its minimum, and $\psi_0(y)$ is the value of the order parameter at the minimum of $F - \mu N$ at a fixed μ. In the gas phase $\psi_0(y) = \sqrt{n}$.

(iii) The square of the roton gap in the Bogoliubov spectrum (9) in the homogeneous phase is given by

$$E_{\mathrm{r}}^2 = \min_{\mathbf{p}} \varepsilon_{\mathbf{p}}^2, \tag{13}$$

with the minimization performed separately for p_x and p_y, starting from the maxon momentum (if it exists).

(iv) The magnitude of the diagonal long-range order (DLRO) for the DW is given by

$$\Gamma = \int_0^{\lambda_0} \frac{(|\psi_0(y)|^2 - n)^2}{n^2} \frac{dy}{\lambda_0}, \tag{14}$$

where λ_0 is the value of the DW period λ at the minimum of $F - \mu N$. At small $(n_{\max} - n_{\min})/n$, from Eq. (14) we obtain

$$\Gamma \approx \frac{(n_{\max} - n_{\min})^2}{8n^2},$$

where $n_{\max}$ and $n_{\min}$ are the respective maximum and minimum values of the quantity $|\psi_0(y)|^2$.

(v) The average density is given by

$$n = \int_0^{\lambda_0} |\psi_0(y)|^2 \frac{dy}{\lambda_0}. \tag{15}$$

(vi) The diagonal elements Y_x and Y_y of the helicity modulus tensor for the superfluid component [82] are given by

$$Y_x = \frac{1}{m^2 S} \frac{d^2 F_0(\mathbf{v})}{dv_x^2}\bigg|_{\mathbf{v}=0}, \quad Y_y = \frac{1}{m^2 S} \frac{d^2 F_0(\mathbf{v})}{dv_y^2}\bigg|_{\mathbf{v}=0}. \tag{16}$$

Here $F_0(\mathbf{v})$ represents the value of F_0 with fixed $\mathbf{v}$. The temperature T_c of the Berezinskii-Kosterlitz-Thouless transition [83] (crossover [84,85]) is determined by the total superfluid density $n_s(T)$ as [86] $T_c = \pi\hbar^2 n_s(T_c)/2m$. The temperature-dependent quantity $n_s \equiv n_s(T)$ can be calculated as the *geometric* mean [87,88] of x and y components of the helicity modulus

$$\frac{n_s}{m} = \sqrt{Y_x Y_y}. \tag{17}$$

(vii) The stretching-compression deformation coefficient u_x and the shear deformation coefficient u_y (which, for the DW, is equivalent to the rotation of the DW) are given by

$$u_x = \frac{1}{S} \frac{d^2 F_0[(1+\beta)\lambda_0]}{d\beta^2}\bigg|_{\beta=0}, \quad u_y = \frac{1}{S} \frac{d^2 F[\psi(\mathrm{R}^\beta \mathbf{r})]}{d\beta^2}\bigg|_{\beta=0}. \tag{18}$$

Here, $F_0(\lambda)$ represents the value of F_0 with fixed λ, and

$$\mathrm{R}^\beta = \begin{pmatrix} \cos(\beta) & \sin(\beta) \\ -\sin(\beta) & \cos(\beta) \end{pmatrix} \tag{19}$$

is the rotation matrix by an angle β. For convenience, we rotate the Hamiltonian with respect to the DW, using the function $U(\mathrm{R}^{-\beta}\mathbf{p})$ instead of $U(\mathbf{p})$.

C. Details of minimization

The ground state of a supersolid, which is characterized by a stationary and undeformed DW, is to be determined

by minimizing the functional $F - \mu N$ with a fixed chemical potential μ [see Eq. (1)], according to the principles of a first-order phase transition. As a result of this procedure, we obtain $\psi_0(y)$, with which we calculate the particle number as $N = \int |\psi_0(y)|^2 dxdy$ for the same μ. Subsequently, while keeping the particle number fixed at N [89], we minimize the functional F with additional constraints imposed on the velocity dv and the deformation $d\beta$. From this minimization, we derive the tensors for the helicity modulus and deformation.

Below we show the results of the numerical minimization of both functionals, F and $F - \mu N$, with the use of the simulated annealing method. To compute the ground state of the supersolid, we start with a random configuration and set the initial "temperature" $\mathcal{T}$ in the Metropolis algorithm to be of the order of $Se_0(n)$. For the calculation of the deformation tensor and the superfluid component, we use the previously determined ground-state profile as the initial configuration. The initial temperature is on the order of $Nm(d\mathbf{v})^2/2$ when calculating the helicity modulus tensor and $Se_0(n)(d\mathbf{a})^2/2$ when computing the deformation tensor. The final temperature is approximately 12–16 orders of magnitude lower than the initial temperature, and the temperature reduction follows a monotonically decreasing exponential trend. The number of iterations is chosen to achieve complete annealing, and poorly annealed calculations in the immediate vicinity of phase transitions are disregarded. For a fine exploration of the first-order phase transition, we employ multiple annealings, initiated from various random configurations.

III. SUPERSOLID DENSITY WAVE

The results presented below numerically indicate the existence of a stable supersolid DW following the scenario of rotonlike attraction with stabilizing many-body repulsion [35] and the decisive role of anisotropy [44]. The calculations are performed for $m = 164$ a.u. and $a_d = 7$ nm, which correspond to dysprosium atoms [5]. The problem is characterized by five dimensionless control parameters:

$$\nu = \frac{a_d}{z_0}, \quad \eta = \frac{\mu m z_0^2}{\hbar^2}, \quad \alpha = \frac{a_s}{a_d}, \quad \alpha_3 = \frac{m g_3}{2\pi\hbar^2 z_0 a_d}, \quad (20)$$

and θ. In all the data, we use the following set of parameters: $\nu = 7/150$, $\eta = 0.0042$, and $\alpha = -3/7$, corresponding to $\mu = 0.76$ nK, $z_0 = 150$ nm, $a_s = -3$ nm, and we work within the variables α_3 and θ.

A. Stable supersolid density wave

According to the numerical calculation with $\alpha_3 = 0.161$ and $\theta = 44.3^\circ$, we clearly observe the effect of a supersolid density wave in a 2D array of tilted dipoles. The squared profile of the order parameter $|\psi_0(y)|^2$ exhibits periodic oscillations with a relative amplitude of $(n_{\max} - n_{\min})/n = 3.2$. The magnitude of DLRO [see Eq. (14)] is $\Gamma = 1.26$, which indicates its nonzero value. Superfluidity is also observed. Both diagonal elements of the helicity modulus tensor in its principal axes, $Y_x = n/m$ and $Y_y = 0.28n/m$, are nonzero. Elasticity is present since the stretching-compression deformation coefficient $u_x = 1.4e_0(n)$m and the shear deformation coefficient $u_y = 2.9e_0(n)$ are both nonzero. Both stability-related

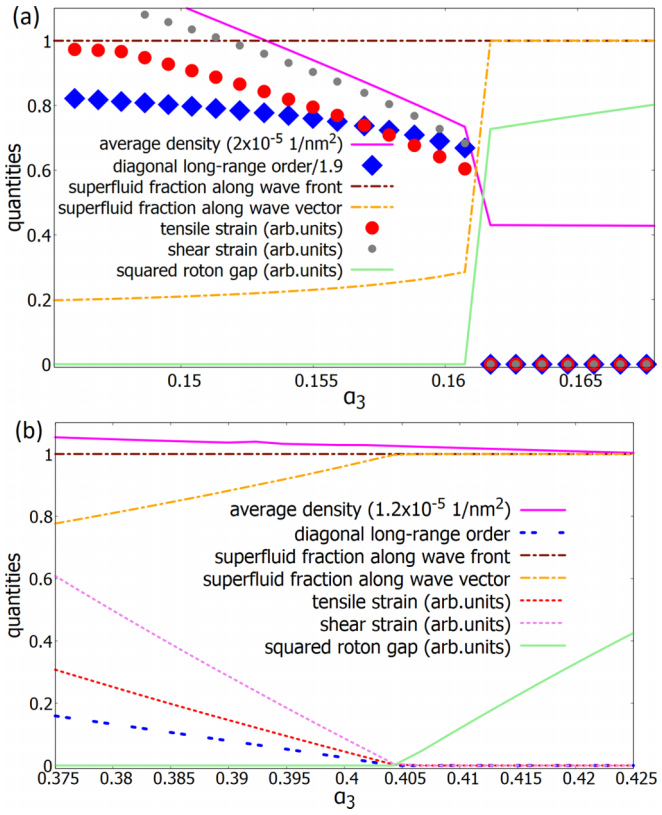

FIG. 2. The (a) first-order gas to supersolid density-wave transition at $\theta = 44.3^\circ$ and the (b) second-order transition at $\theta = 46^\circ$ are illustrated. Both components of the helicity modulus tensor, Y_x and Y_y, and the deformation tensor, u_x and u_y, are shown, along with the diagonal long-range order parameter Γ, the square of the roton gap E_r^2, and the average density n. The first-order (second-order) transition corresponds to the jump in panel (a) [kink in panel (b)].

quantities, the compressibility $m^2/\chi = 0.0053(4\pi\hbar^2/m)$ and the pressure $P = 10.2e_0(n)$, are positive. Finally, in the 2D weakly correlated system at $T = 0$, a Bose-Einstein condensate is indeed present, and its existence does not require further verification. To conclude, we see all the features of the supersolid phase.

We summarize our results in phase diagrams, which are presented in Fig. 2. As is known, in the 2D isotropic case, the gas-supersolid transition is of the first order [35]. Therefore, even with a sufficiently weak anisotropy, the nature of this transition should be of the first kind. This is precisely evident in Fig. 2(a): at the tilt angle $\theta = 44.3^\circ$, the magnitude of the DLRO and both components of the strain and helicity modulus tensors, as well as the square of the roton gap and the average density, undergo abrupt changes at the transition point.

However, with increasing anisotropy, i.e., with the growth of the tilt angle θ, the magnitudes of these jumps *decrease*, as it is illustrated in Fig. 3(a). At the certain critical value $\theta_c = 45.3^\circ$, all jumps simultaneously *vanish*. With further increase in anisotropy at angles $\theta > \theta_c$, only *kinks* are present instead of jumps. These kinks indicate a second-order transition, as shown in Fig. 2(b). The phase diagram of the gas-supersolid transition has a point of intersection between

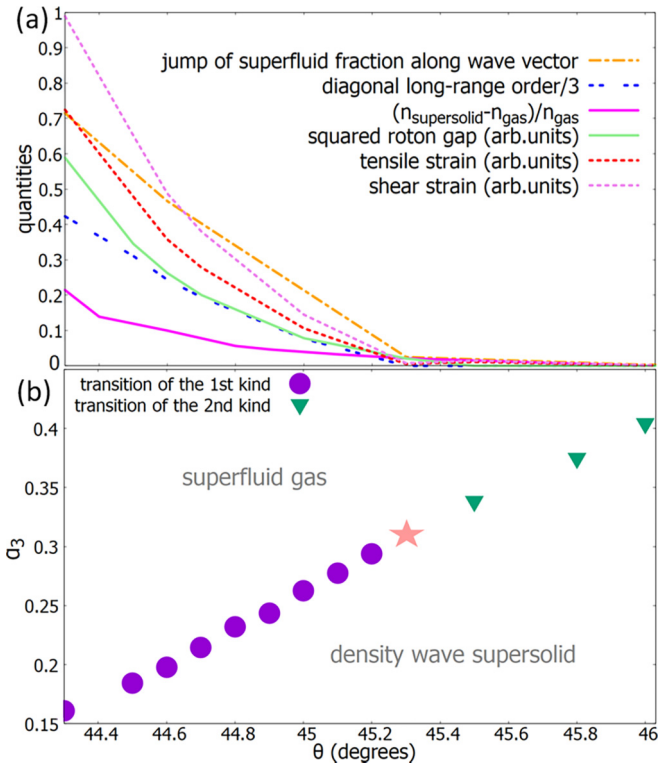

FIG. 3. In panel (a), the jump magnitudes at the transition are shown for the Y_y component of the helicity modulus, both components u_x and u_y of the strain tensor, the DLRO magnitude Γ, the density jump between supersolid and gas, and the square of the roton gap E_r^2, as functions of the tilt angle θ. (b) The phase diagram of the θ-α_3 variables is presented. The pink star denotes the intersection point of the first- and second-order transitions.

the first- and second-order transitions at $\theta = \theta_c$ [see Fig. 3(b)]: the first-order transition for weaker anisotropy ($\theta < \theta_c$) and the second-order transition for stronger anisotropy ($\theta > \theta_c$).

IV. LHY CORRECTION

Up to this point, we have considered a model case of the stabilization by three-body interactions. However, for atoms, an experimentally interesting scenario involves many-body stabilization via the LHY correction. Therefore, below we derive the equation of state $e_0(n)$ with the LHY correction instead of Eq. (2) and minimize the free energy functional (1), specifically with this $e_0(n)$.

A. Relations

We start with the three-dimensional interaction Hamiltonian incorporating the LHY correction:

$$\hat{H}_{\rm int} = \frac{1}{2}\int d\vec{r}\, d\vec{s}\; \mathcal{U}_{\rm 3D}(\vec{r}-\vec{s})\hat{\Psi}^+(\vec{r})\hat{\Psi}^+(\vec{s})\hat{\Psi}(\vec{s})\hat{\Psi}(\vec{r}) + \int d\vec{r}\; e^{\rm 3D}_{\rm LHY}(\hat{\Psi}^+(\vec{r})\hat{\Psi}(\vec{r})). \tag{21}$$

Here $\vec{r} = \{x, y, z\}$, and

$$\mathcal{U}_{\rm 3D}(\vec{r}\,) = \frac{d^2}{\vec{r}^{\,5}}[\vec{r}^{\,2} - 3(x\sin\theta + z\cos\theta)^2] \tag{22}$$

represents the dipole-dipole interaction potential with a tilt, and the last term is given by

$$e^{\rm 3D}_{\rm LHY}(n_{3d}) = \frac{g^{\rm 3D}_s}{2}n^2_{\rm 3D} + \frac{2}{5}g^{\rm 3D}_{\rm LHY}n^{5/2}_{\rm 3D}, \tag{23}$$

where the quantity

$$g^{\rm 3D}_s = \frac{4\pi\hbar^2 a_s}{m} \tag{24}$$

corresponds to the three-dimensional s-wave scattering, and the quantity [80]

$$g^{\rm 3D}_{\rm LHY} = \frac{128}{3m}\hbar^2 a_s^{5/2}\left[1 + \frac{3}{2}\left(\frac{a_d}{a_s}\right)^2\right] \tag{25}$$

is responsible for the LHY correction.

In contrast to Sec. III, physical parameters for numerical estimation, as observed in Sec. IV B, occur in the crossover regime with μ several times larger than $\hbar\omega_z$. To tackle such a problem, we approximate by separating variables z and $\mathbf{r}$ for the lowest branch of the 3D field operator, and we write

$$\hat{\Psi}(\vec{r}\,) \approx \varphi(z)\hat{\Psi}(\mathbf{r}) + \hat{\Psi}_1(\vec{r}\,). \tag{26}$$

Here, the 2D field $\hat{\Psi}(\mathbf{r})$ and the wave function $\varphi(z)$ correspond to the lowest branch, while in $\hat{\Psi}_1(\vec{r})$, all excited branches are combined.

Further, we make the following two simplifications.

(i) At low temperatures ($T \lesssim \mu$) and weak interactions ($n - n_0 \ll n_0$), the excited modes are weakly populated, allowing us to neglect the contribution of $\hat{\Psi}_1(\vec{r}\,)$, because it corresponds to the noncondensed fraction [90].

(ii) For values of μ only a few times larger than $\hbar\omega_z$, we can still approximately assume that the wave function $\varphi(z)$ has a Gaussian profile with an oscillation frequency of the order of the trap frequency [91].

As a result of these simplifications, we obtain

$$\varphi(z) \approx \exp\left(-z^2/2z_0^2\right)/\sqrt{\sqrt{\pi}z_0}, \quad \hat{\Psi}_1(\vec{r}) \approx 0. \tag{27}$$

Subsequently, all considerations are analogous to those in Ref. [44] and lead to the same Hamiltonian as Eq. (1), with the exception that instead of formula (2), we obtain

$$e_0(n) = \frac{g_2}{2}n^2 + \frac{2g_{\rm LHY}}{5}n^{5/2} + \cdots, \tag{28}$$

where g_2 is defined in Sec. II and Ref. [92], and

$$g_{\rm LHY} = g^{\rm 3D}_{\rm LHY}\sqrt{\tfrac{2}{5}}z_0^{-\frac{3}{2}}\pi^{-\frac{1}{4}}. \tag{29}$$

In this approach, three-body interactions are not considered at all ($g_3 = 0$).

B. Results

In all subsequent results, we use the following values: $\mu =$ 33 nK, $z_0 = 500$ nm, while the adjustable parameters are α and θ.

We observe that LHY stabilization in a wide layer results in a supersolid phase exhibiting both first- and second-order transitions, as depicted in Fig. 4.

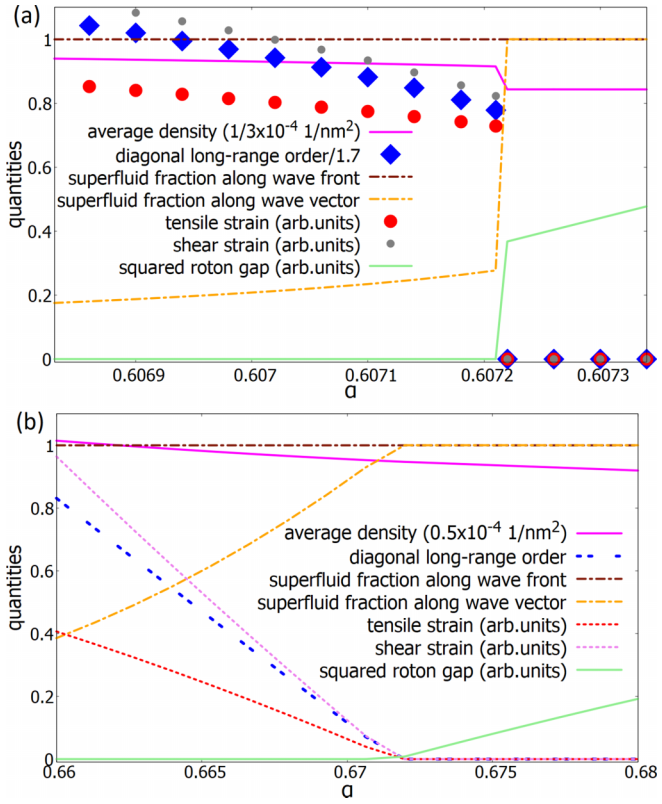

FIG. 4. (a) First-order gas to supersolid density-wave transition at $\theta = 56.6^\circ$ and (b) second-order transition at $\theta = 64^\circ$ are illustrated. Both components of the helicity modulus tensor, Y_x and Y_y, and the deformation tensor, u_x and u_y, are shown, along with the diagonal long-range order parameter Γ, the square of the roton gap E_r^2, and the average density n. The first-order (second-order) transition corresponds to the jump in panel (a) [kink in panel (b)].

In the phase diagram (Fig. 5), the point of intersection between the first- and second-order transitions is clearly visible. As the anisotropy increases (with the tilting angle θ), the supersolid effect intensifies: the superfluid transitions into a supersolid. Additionally, with the increasing influence of many-body effects [i.e., with increasing α, see Eqs. (25) and (29)], the system moves from a first-order transition to a second-order transition. The same takes place with the increase of anisotropy [i.e., with increasing θ].

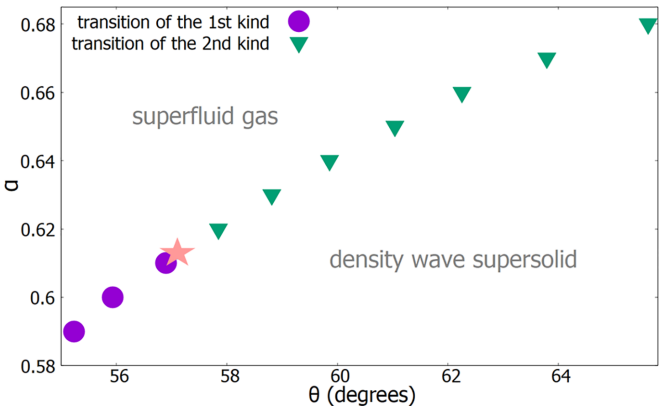

FIG. 5. The phase diagram of the θ-α variables is presented. The pink star denotes the intersection point of first- and second-order transitions.

Thus, the scenario for a supersolid stabilized by LHY is totally analogous to the previously examined model situation with stabilization by three-body interactions.

V. DISCUSSION AND CONCLUSION

Let us consider the case of finite temperature. Due to the infrared divergence of the Hohenberg type [93] in a macroscopic system, there exists a quasicondensate with superfluidity instead of a Bose-Einstein condensate. Also, there is no macroscopic long-range order, only quasi-long-range order and elasticity [83,94]. Furthermore, at nonzero temperature, the mechanism responsible for the convergence of condensate depletion for the second-order transition, as described in Ref. [44], will be disrupted. Nonetheless, this is not a significant concern as the system will still be within a regime of weak correlations. Additionally, near the zero-touch spectrum, the gas will already exhibit a local density wave due to the redistribution of population from $k = 0$ to modes with $\mathbf{k} \approx \pm\mathbf{k}_{\rm roton}$. Therefore, at sufficiently low temperatures, it is plausible that second-order transitions may become first-order transitions, albeit with small jumps (at low temperatures and/or a thick layer). The calculation is nontrivial and warrants further research.

In this work, we have presented the results of the investigation of the supersolidity effect in the system of tilted dipolar bosons with stabilizing many-body repulsion. We have examined both model stabilization by the three-body interactions and by the LHY term. We have identified the second-order transition from gas to density-wave-type supersolid and the point of intersection with the first-order transition line appears to be a general feature in 2D at $T = 0$ and inherently arises from the anisotropy of the system. The observed pattern of first- and second-order transitions in the gas-supersolid transition for anisotropic 2D systems aligns with the touching of the Bogoliubov spectrum zero-energy points at two-roton momenta $\pm\mathbf{k}_{\rm roton}$ [44]. Indeed, the zero-roton gap allows for the *macroscopic population transfer* from the homogeneous condensate to these two states due to the touching. Consequently, the superposition leads to the density wave of the condensate: $\psi(\mathbf{r}) = a_0 + a_1 \cos(\mathbf{k}_{\rm roton}\mathbf{r}) + \cdots$. Moreover, the absence of Fischer-like [41] divergence beyond the condensate under the conditions of roton gap closing at two points [44] allows the system to remain within the regime of weak correlations.

As we expected, the proposed approach can be used in ongoing experiments on the study of supersolidity of dipolar bosons. In particular, in the experiment with untilted dipoles ($\theta = 0$), but in a cigar-shaped trap [95], a point of the intersection between first- and second-order transitions in the gas-supersolid transition has also been observed (this is consistent with the theory provided in Refs. [66,95]). In this experiment, the anisotropy is imposed by the geometry: DWs are indeed formed along the cigar. In our case, in the 2D system anisotropy can be imposed by the control of the electric field in the case of polar molecules [1–3] or an external magnetic field for ultracold atoms with induced dipole moment, such as erbium [7] or dysprosium [5,6]. Finally, we

expect qualitatively similar results regarding the supersolid of density waves for excitonic realizations in both monolayers of transition metal dichalcogenides [13] and GaAs quantum wells [96].

ACKNOWLEDGMENTS

The work of Yu.E.L. is supported by the Russian Science Foundation under Grant No. 23-12-00115 (studying supersolid states). A.K.F. acknowledges the support by the Russian Science Foundation under Grant No. 19-71-10092 (analysis of the phase diagram) and the Priority 2030 program at the National University of Science and Technology "MISIS" under Project No. K1-2022-027. I.L.K. acknowledges the support of Project No. FFUU-2024-0003 of the Institute of Spectroscopy of the Russian Academy of Sciences. The work was also supported by the Russian Roadmap on Quantum Computing (Contract No. 868-1.3-15/15-2021).

[1] L. D. Carr, D. DeMille, R. V. Krems, and J. Ye, New J. Phys. **11**, 055049 (2009).
[2] O. Dulieu and C. Gabbanini, Rep. Prog. Phys. **72**, 086401 (2009).
[3] S. A. Moses, J. P. Covey, M. T. Miecnikowski, D. S. Jin, and J. Ye, Nat. Phys. **13**, 13 (2017).
[4] A. Griesmaier, J. Werner, S. Hensler, J. Stuhler, and T. Pfau, Phys. Rev. Lett. **94**, 160401 (2005).
[5] M. Lu, N. Q. Burdick, S. H. Youn, and B. L. Lev, Phys. Rev. Lett. **107**, 190401 (2011).
[6] M. Lu, N. Q. Burdick, and B. L. Lev, Phys. Rev. Lett. **108**, 215301 (2012).
[7] K. Aikawa, A. Frisch, M. Mark, S. Baier, A. Rietzler, R. Grimm, and F. Ferlaino, Phys. Rev. Lett. **108**, 210401 (2012).
[8] A. V. Gorbunov and V. B. Timofeev, JETP Lett. **84**, 329 (2006).
[9] E. Tutuc and D. W. Snoke, Adv. Condens. Matter Phys. **2011**, 938609 (2011).
[10] A. A. High, J. R. Leonard, A. T. Hammack, M. M. Fogler, L. V. Butov, A. V. Kavokin, K. L. Campman, and A. C. Gossard, Nature (London) **483**, 584 (2012).
[11] Y. Shilo, K. Cohen, B. Laikhtman, K. West, L. Pfeiffer, and R. Rapaport, Nat. Commun. **4**, 2335 (2013).
[12] A. K. Geim and I. V. Grigorieva, Nature (London) **499**, 419 (2013).
[13] M. M. Fogler, L. V. Butov, and K. S. Novoselov, Nat. Commun. **5**, 4555 (2014).
[14] M. Alloing, M. Beian, M. Lewenstein, D. Fuster, Y. Gonzalez, L. Gonzalez, R. Combescot, M. Combescot, and F. Dubin, Europhys. Lett. **107**, 10012 (2014).
[15] Yu. E. Lozovik and V. I. Yudson, Pis'ma Zh. Éksp. Teor. Fiz. **22**, 556 (1975) [Sov. JETP Lett. **22**, 274 (1975)].
[16] Y. Lozovik and V. Yudson, Phys. A (Amsterdam, Neth.) **93**, 493 (1978).
[17] Y. Lozovik and V. Mandelshtam, Phys. Lett. A **138**, 204 (1989).
[18] M. Marinescu and L. You, Phys. Rev. Lett. **81**, 4596 (1998).
[19] L. Santos, G. V. Shlyapnikov, P. Zoller, and M. Lewenstein, Phys. Rev. Lett. **85**, 1791 (2000).
[20] M. Baranov, Phys. Rep. **464**, 71 (2008).
[21] T. Lahaye, C. Menotti, L. Santos, M. Lewenstein, and T. Pfau, Rep. Prog. Phys. **72**, 126401 (2009).
[22] M. A. Baranov, M. Dalmonte, G. Pupillo, and P. Zoller, Chem. Rev. **112**, 5012 (2012).
[23] Y. E. Lozovik, Phys.-Usp. **61**, 1094 (2018).
[24] L. Chomaz, I. Ferrier-Barbut, F. Ferlaino, B. Laburthe-Tolra, B. L. Lev, and T. Pfau, Rep. Prog. Phys. **86**, 026401 (2023).
[25] S. Balibar, Nature (London) **464**, 176 (2010).
[26] A. B. Kuklov, N. V. Prokof'ev, and B. V. Svistunov, Physics **4**, 109 (2011).
[27] M. Boninsegni and N. V. Prokof'ev, Rev. Mod. Phys. **84**, 759 (2012).
[28] S. Balibar, A. D. Fefferman, A. Haziot, and X. Rojas, J. Low Temp. Phys. **168**, 221 (2012).
[29] V. I. Yukalov, Physics **2**, 49 (2020).
[30] A. Recati and S. Stringari, Nat. Rev. Phys. **5**, 735 (2023).
[31] E. P. Gross, Phys. Rev. **106**, 161 (1957).
[32] A. F. Andreev and I. M. Lifshitz, Sov. Phys.-Usp. **13**, 670 (1971).
[33] D. Kirzhnits and Y. Nepomnyashchii, Zh. Eksp. Teor. Fiz. **59**, 2203 (1970) [Sov. Phys. JETP **32**, 1191 (1971)].
[34] Y. Pomeau and S. Rica, Phys. Rev. Lett. **72**, 2426 (1994).
[35] Z.-K. Lu, Y. Li, D. S. Petrov, and G. V. Shlyapnikov, Phys. Rev. Lett. **115**, 075303 (2015).
[36] H. Saito, Y. Kawaguchi, and M. Ueda, Phys. Rev. Lett. **102**, 230403 (2009).
[37] H. P. Buchler and G. Blatter, Phys. Rev. Lett. **91**, 130404 (2003).
[38] S. Yi, T. Li, and C. P. Sun, Phys. Rev. Lett. **98**, 260405 (2007).
[39] I. Danshita and C. A. R. Sá de Melo, Phys. Rev. Lett. **103**, 225301 (2009).
[40] L. Santos, G. V. Shlyapnikov, and M. Lewenstein, Phys. Rev. Lett. **90**, 250403 (2003).
[41] U. R. Fischer, Phys. Rev. A **73**, 031602(R) (2006).
[42] S. Komineas and N. R. Cooper, Phys. Rev. A **75**, 023623 (2007).
[43] A. Boudjemâa and G. V. Shlyapnikov, Phys. Rev. A **87**, 025601 (2013).
[44] A. K. Fedorov, I. L. Kurbakov, Y. E. Shchadilova, and Y. E. Lozovik, Phys. Rev. A **90**, 043616 (2014).
[45] F. Cinti, P. Jain, M. Boninsegni, A. Micheli, P. Zoller, and G. Pupillo, Phys. Rev. Lett. **105**, 135301 (2010).
[46] N. Henkel, R. Nath, and T. Pohl, Phys. Rev. Lett. **104**, 195302 (2010).
[47] A. E. Golomedov, G. E. Astrakharchik, and Y. E. Lozovik, Phys. Rev. A **84**, 033615 (2011).
[48] S. Saccani, S. Moroni, and M. Boninsegni, Phys. Rev. B **83**, 092506 (2011).
[49] H. P. Büchler, E. Demler, M. Lukin, A. Micheli, N. Prokof'ev, G. Pupillo, and P. Zoller, Phys. Rev. Lett. **98**, 060404 (2007).
[50] G. E. Astrakharchik, J. Boronat, I. L. Kurbakov, and Y. E. Lozovik, Phys. Rev. Lett. **98**, 060405 (2007).
[51] D. M. Ceperley and B. Bernu, Phys. Rev. Lett. **93**, 155303 (2004).

[52] M. Boninsegni, A. B. Kuklov, L. Pollet, N. V. Prokof'ev, B. V. Svistunov, and M. Troyer, Phys. Rev. Lett. **97**, 080401 (2006).

[53] M. Boninsegni, N. Prokof'ev, and B. Svistunov, Phys. Rev. Lett. **96**, 105301 (2006).

[54] L. Pollet, M. Boninsegni, A. B. Kuklov, N. V. Prokof'ev, B. V. Svistunov, and M. Troyer, Phys. Rev. Lett. **98**, 135301 (2007).

[55] I. L. Kurbakov, Y. E. Lozovik, G. E. Astrakharchik, and J. Boronat, Phys. Rev. B **82**, 014508 (2010).

[56] E. Burovski, E. Kozik, A. Kuklov, N. Prokof'ev, and B. Svistunov, Phys. Rev. Lett. **94**, 165301 (2005).

[57] A. S. C. Rittner and J. D. Reppy, Phys. Rev. Lett. **97**, 165301 (2006).

[58] S. Sasaki, R. Ishiguro, F. Caupin, H. J. Maris, and S. Balibar, Science **313**, 1098 (2006).

[59] R. M. Wilson, S. Ronen, J. L. Bohn, and H. Pu, Phys. Rev. Lett. **100**, 245302 (2008).

[60] R. M. Wilson, C. Ticknor, J. L. Bohn, and E. Timmermans, Phys. Rev. A **86**, 033606 (2012).

[61] D. S. Petrov, Phys. Rev. Lett. **115**, 155302 (2015).

[62] Y.-C. Zhang and F. Maucher, Atoms **11**, 102 (2023).

[63] C. Mishra and R. Nath, Phys. Rev. A **94**, 033633 (2016).

[64] L. Chomaz, R. M. W. van Bijnen, D. Petter, G. Faraoni, S. Baier, J. H. Becher, M. J. Mark, F. Wächtler, L. Santos, and F. Ferlaino, Nat. Phys. **14**, 442 (2018).

[65] D. Petter, G. Natale, R. M. W. van Bijnen, A. Patscheider, M. J. Mark, L. Chomaz, and F. Ferlaino, Phys. Rev. Lett. **122**, 183401 (2019).

[66] P. B. Blakie, D. Baillie, L. Chomaz, and F. Ferlaino, Phys. Rev. Res. **2**, 043318 (2020).

[67] M. A. Norcia, C. Politi, L. Klaus, E. Poli, M. Sohmen, M. J. Mark, R. N. Bisset, L. Santos, and F. Ferlaino, Nature (London) **596**, 357 (2021).

[68] M. Wenzel, F. Böttcher, T. Langen, I. Ferrier-Barbut, and T. Pfau, Phys. Rev. A **96**, 053630 (2017).

[69] L. Chomaz, D. Petter, P. Ilzhöfer, G. Natale, A. Trautmann, C. Politi, G. Durastante, R. M. W. van Bijnen, A. Patscheider, M. Sohmen, M. J. Mark, and F. Ferlaino, Phys. Rev. X **9**, 021012 (2019).

[70] L. Tanzi, E. Lucioni, F. Famà, J. Catani, A. Fioretti, C. Gabbanini, R. N. Bisset, L. Santos, and G. Modugno, Phys. Rev. Lett. **122**, 130405 (2019).

[71] F. Böttcher, J.-N. Schmidt, M. Wenzel, J. Hertkorn, M. Guo, T. Langen, and T. Pfau, Phys. Rev. X **9**, 011051 (2019).

[72] A. Macia, D. Hufnagl, F. Mazzanti, J. Boronat, and R. E. Zillich, Phys. Rev. Lett. **109**, 235307 (2012).

[73] R. Bombin, J. Boronat, and F. Mazzanti, Phys. Rev. Lett. **119**, 250402 (2017).

[74] R. Bombín, F. Mazzanti, and J. Boronat, Phys. Rev. A **100**, 063614 (2019).

[75] F. Cinti and M. Boninsegni, J. Low Temp. Phys. **196**, 413 (2019).

[76] F. Cinti and M. Boninsegni, Phys. Rev. A **102**, 047301 (2020).

[77] R. Bombín, F. Mazzanti, and J. Boronat, Phys. Rev. A **102**, 047302 (2020).

[78] D. S. Petrov, Phys. Rev. Lett. **112**, 103201 (2014).

[79] A. R. P. Lima and A. Pelster, Phys. Rev. A **84**, 041604(R) (2011).

[80] A. R. P. Lima and A. Pelster, Phys. Rev. A **86**, 063609 (2012).

[81] H.-W. Hammer, A. Nogga, and A. Schwenk, Rev. Mod. Phys. **85**, 197 (2013).

[82] Y. E. Lozovik, I. L. Kurbakov, and P. A. Volkov, Phys. Rev. B **95**, 245430 (2017).

[83] J. M. Kosterlitz and D. J. Thouless, J. Phys. C **6**, 1181 (1973).

[84] Y. E. Lozovik, I. Kurbakov, and M. Willander, Phys. Lett. A **366**, 487 (2007).

[85] N. S. Voronova, I. L. Kurbakov, and Y. E. Lozovik, Phys. Rev. Lett. **121**, 235702 (2018).

[86] D. R. Nelson and J. M. Kosterlitz, Phys. Rev. Lett. **39**, 1201 (1977).

[87] P. Minnhagen and P. Olsson, Phys. Rev. B **44**, 4503 (1991).

[88] J.-S. You, H. Lee, S. Fang, M. A. Cazalilla, and D.-W. Wang, Phys. Rev. A **86**, 043612 (2012).

[89] M. E. Fisher, M. N. Barber, and D. Jasnow, Phys. Rev. A **8**, 1111 (1973).

[90] A. Griffin, Phys. Rev. B **53**, 9341 (1996).

[91] We numerically solved the Gross-Pitaevskii equation (without both the LHY correction and the noncontact part in $\mathbf{r}-\mathbf{s}$) [97], finding that, at $\mu = 33$ nK, the oscillator frequency $\hbar\omega_z = 12$ nK is reproduced for a trap frequency of 25 nK. The latter is compared with μ. Moreover, the Gaussian $\varphi(z)$ and the ground-state wave function of the GP equation $\psi_{\rm GS}(z)$ after a normalization by $\int_{-\infty}^{+\infty}|\varphi(z)|^2dz = \int_{-\infty}^{+\infty}|\psi_{\rm GS}(z)|^2dz$ differ in amplitude by only 0.5% in between, while the profiles $|\varphi(z)|^2$ and $|\psi_{\rm GS}(z)|^2$ differ in absolute units by less than 5%.

[92] B. T. E. Ripley, D. Baillie, and P. B. Blakie, Phys. Rev. A **108**, 053321 (2023).

[93] P. C. Hohenberg, Phys. Rev. **158**, 383 (1967).

[94] V. L. Berezinsky, Zh. Eksp. Teor. Fiz. **59**, 907 (1971) [Sov. Phys. JETP **32**, 493 (1971)].

[95] G. Biagioni, N. Antolini, A. Alana, M. Modugno, A. Fioretti, C. Gabbanini, L. Tanzi, and G. Modugno, Phys. Rev. X **12**, 021019 (2022).

[96] A. K. Fedorov, I. L. Kurbakov, and Y. E. Lozovik, Phys. Rev. B **90**, 165430 (2014).

[97] G. Baym and C. J. Pethick, Phys. Rev. Lett. **76**, 6 (1996).